Current Optics and Photonics
Vol. 4, No. 1, February 2020, pp. 44-49

ISSN: 2508-7266(Print) / ISSN: 2508-7274(Online)
DOI: https://doi.org/10.3807/COPP.2020.4.1.044

A New Method for Measuring Refractive Index with a Laser Frequency-shifted Feedback Confocal Microscope

Borui Zhou[1]*, Zihan Wang[2], and Xueju Shen[1]

[1]*Department of Electronic and Optical Engineering, Army Engineering University of PLA, Shijiazhuang 050051, China*
[2]*College of Science, Beijing Forestry University, Beijing 100083, China*

(Received September 25, 2019 : revised October 25, 2019 : accepted November 1, 2019)

In this paper, a new method is presented to measure the refractive index of single plain glass or multilayered materials, based on a laser frequency-shifted confocal feedback microscope. Combining the laser frequency-shifted feedback technique and the confocal effect, the method can attain high axial-positioning accuracy, stability and sensitivity. Measurements of different samples are given, including N-BK7 glass, Silica plain glass, and a microfluidic chip with four layers. The results for N-BK7 glass and Silica plain glass show that the measurement uncertainty in the refractive index is better than 0.001. Meanwhile, the feasibility of this method for multilayered materials is tested. Compared to conventional methods, this system is more compact and has less difficulty in sample processing, and thus is promising for applications in the area of refractive-index measurement.

Keywords : Refractive index, Optical measurement, Laser frequency-shifted feedback, Confocal effect
OCIS codes : (120.0120) Instrumentation, measurement and metrology; (140.0140) Lasers and laser optics; (180.1790) Confocal microscopy; (180.0180) Microscopy

I. INTRODUCTION

Accurate measurement of refractive index is significant in various applications, such as the design of binary optical elements and in the identification of various biomaterials. The existing methods for refractive-index measurement primarily include the Abbe refractometer [1, 2], the minimum-deviation method [3-5], ellipsometry [6-8], the *m*-lines method [9-11], interferometry [12-17], and surface plasmon resonance [18-20]. The Abbe refractometer is widely used in manufacturing and laboratory settings, offering a superior accuracy of 10^{-4}, but its measurement range of refractive index is limited by total reflection. Although the accuracy of the minimum-deviation method can be up to 10^{-6}, measurement accuracy relies on the machining precision of the apex angle. In addition, this method is not suitable for practical use, due to its costly sample processing, huge instrument, and strict environmental conditions. Ellipsometry is appropriate for measuring the refractive indices of thin films and bulk media, but its measurement accuracy is only 10^{-2} [8]. Another way to measure the refractive index of a thin film is the *m*-lines method which can provide an accuracy of 10^{-3} [11]; in comparison, interferometry can measure refractive index and thickness of an optical material simultaneously, with an accuracy of up to 10^{-5} [16, 17].

Laser frequency-shifted feedback was first reported by K. Otsuka in 1979 [21], and since has been widely used in the fields of displacement measurement [22-24], velocity measurement [25], and vibration measurement [26], because of its high sensitivity, simple pumping scheme, and automatic alignment. Considering the high sensitivity of the laser frequency-shifted feedback effect, it has great potential for detection of the weak light intensity reflected by an interface with a very low difference in reflectivity index. Laser feedback interferometry has been used for

*Corresponding author: zbr15601587718@163.com, ORCID 0000-0001-7908-0442
Color versions of one or more of the figures in this paper are available online.

glass reflectivity-index and thickness measurement [21, 22], based on the optical-path difference caused by rotating the sample; herefore, it does not apply to refractive-index measurement of multilayered media or liquids.

Combining the confocal effect and laser frequency-shifted feedback, here a new method for refractive-index measurement is presented, which is noncontact, highly sensitive, and can accommodate multilayered media and liquids. In this method, the sample is scanned by a laser-frequency-shifted feedback confocal microscope along the optical axis, and the interfaces generated by different refractive indices correspond to the peaks of the scanning curve. Then the optical thickness is calculated with the known stage movement between the two peaks, and ray analysis. Finally, the ratio of the optical thickness to the physical thickness is used to calculate the refractive index. Compared to conventional methods, this technique is more compact and has less difficulty with sample processing. In particular, the laser-frequency-shifted feedback confocal microscope is extremely sensitive, and the amplification coefficient provided by laser feedback technology can reach 10^6, which means that this method can measure the refractive indices of multilayered media with very low refractive-index differences. Thus it is a promising technique for refractive-index measurement.

II. EXPERIMENTAL SETUP AND PRINCIPLE

2.1. Laser Frequency-shifted Feedback Confocal Microscope

The system configuration of the laser frequency-shifted feedback confocal microscope is shown in Fig. 1. The *a*-cut Nd:YVO_4 microchip laser (ML) pumped by a laser diode (VLSP-808-B-SF, Connect) is chosen as the light source; the microchip is 0.75 mm thick. The laser emits a single longitudinal mode and linearly polarized beam of wavelength 1064 nm. The light is then split into two identical beams by the beam splitter (BS); the reflected beam is received by the photodetector (PD) for signal detection and demodulation, while the transmitted one is injected into acousto-optic frequency shifters (AOFSs). In the measurement optical path, two acousto-optic frequency shifters are aligned in a differential configuration, and the light passing through AOFS1 and AOFS2 is divided into four beams. The beam with a frequency shift of Ω induced by AOFS1's +1-order diffraction and AOFS2's -1-order diffraction serves as the measuring light. In the experiment, AOFS1 and AOFS2 are driven at ω_1=70MHz and $\omega_2 = 71MHz$ respectively, producing a frequency shift of $\Omega=|\omega_1-\omega_2|$.

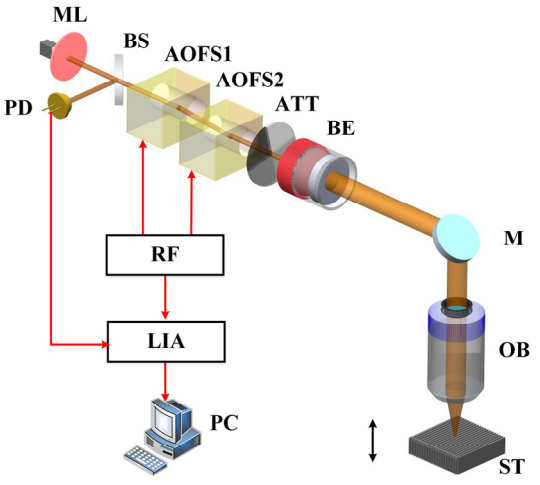

FIG. 1. Experimental system of LFCT and LCT. ML: microchip laser; BS: beam splitter; PD: photon detector; ATT: attenuator; AOFS: acousto-optic frequency shifter; BE: beam expander; OB: objective; M: mirror; RF: reference signal generator; ST: stage; LIA: lock-in amplifier; PC: computer.

After that, the measuring light is expanded by a beam expander (BE) with an expanding ratio of 10, then focused by a 50× near-infrared objective lens (OB). Specifically, the OB with a numerical aperture (NA) of 0.42 has a long working distance, up to 20.4 mm, for large-scale scanning. A three-dimensional precision stage (XWJ-R, SYMC) is used to scan the sample. It should be noted that there exists a conjugate relationship between the focal point of the OB and the laser-beam waist: The beam waist acts as the equivalent of a spatial pinhole filter, approximately 26 μm in diameter.

The light reflected from the sample returns to the cavity via the original path. In this process, the light has undergone two frequency shifts, causing a total frequency shift of the laser of 2Ω=2MHz. The measurement signal transferred from the PD and the reference signal generated by the mixer are simultaneously input to a lock-in amplifier (LIA) (HF2LI, Zurich Instruments). Finally the LIA demodulates the measurement signal at 2Ω. According to the rate-equation model and confocal effect, the power modulation of laser-frequency-shifted confocal tomography is given by [27, 28]

$$\frac{\Delta I(2\Omega)}{I_S} = \kappa T(z) G(2\Omega)\cos(2\Omega t - \phi - \phi_s),$$
$$T(z) = \left|\frac{\sin kz(1-\sqrt{1-NA^2})}{kz(1-\sqrt{1-NA^2})}\right|^2, \quad G(2\Omega) \approx \frac{2}{\eta}(\gamma_c/\gamma), \tag{1}$$

where ΔI denotes the power-modulation signal of the laser, I_S is the laser's output power in the steady state, κ represents the reflectivity of the sample, $T(z)$ is the defocusing curve, NA is the numerical aperture of the objective lens, $k = 2\pi/\lambda$ is the laser's wave number (with λ being the laser's wavelength), $G(2\Omega)$ is the gain generated by the microchip laser feedback effect, ϕ_s is a fixed additional phase, ϕ is the external cavity feedback phase (which reflects the changes in the outer cavity

length), and $\eta = N_0/N$ is the relative pump level, indicated as the ratio of the actual pump power to the threshold pump power.

The amplification coefficient $G(2\Omega)$ is contingent on the frequency shift 2Ω and the relaxation frequency. When the shifted frequency 2Ω is set close to the relaxation frequency, $G(2\Omega)$ can reach 10^6. This amplification can be utilized in the detection of low-reflection interfaces. Theoretically, when the external cavity reflection coefficient κ reaches the order of 10^{-8}, a modulation depth of 1% can be obtained. This means that, as long as the frequency shift is properly selected, the LFCT system can achieve extremely high detection sensitivity without using high-gain detectors.

2.2. Principle of Refractive-index Measurement

We obtained measurements of the refractive indices of single plain glass and multilayered materials, using the laser-frequency-shifted feedback confocal microscope to track the shift in focal length shift that results from translating the focus along the optical axis within a material of different refractive index. Through analysis of the focused ray after entering the non-air medium, we determined the specific incident angle corresponding to the peak value of the scanning curve, and eliminated the influence of monochromatic aberration. Compared to conventional techniques, this method is more sensitive, more convenient, and has less difficulty in sample processing.

The measurement information comes directly from the axial scan, or indirectly from the tomographic image. During vertical scanning, the laser beam focused by OB is regarded as an optical probe passing through the measured sample. The detected time-domain signal waveform can be represented by Eq. (1), and the envelope of this signal that is demodulated by the LIA (namely, the defocusing curve) is shown in Fig. 2. The peak position of the defocusing curve corresponds exactly to the focus of the optical probe; when the focus of the optical probe touches the sample's surface or an interface, the curve can reach its peak value.

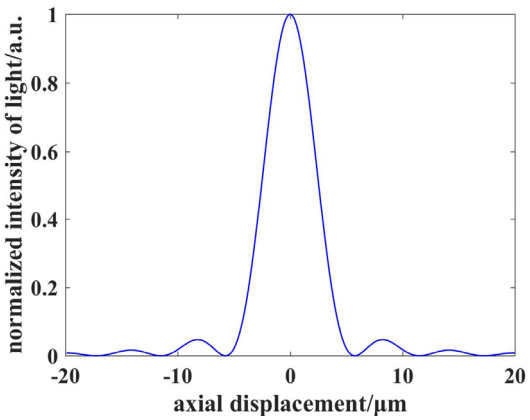

FIG. 2. Defocusing curve of the laser frequency-shifted feedback microscope.

Of particular note is that all light emitted from the objective lens in the air converges in focus, but monochromatic aberration along the optical axis will be produced, and the actual focus will move after the optical probe penetrates the sample, due to the change in refractive index. This process is shown in Fig. 3. The refractive index of the media on both sides of the interface are n_1 and n_2. The incident and refracted angles of the light are α, β. D and L denote respectively the distance from the focus of the incident ray and the focus of the refracted ray to the interface of media. According to Fig. 3, the refractive index n_2 can be expressed as

$$n_2(\alpha) = \frac{n_1 \sin\alpha}{\sin\left(\arctan\left(D\tan\alpha/L\right)\right)}. \tag{2}$$

The refractive index n_2 is rel to the incidence angle α; thus it is significant to find the incidence angle that corresponds to the peak of the defocusing curve. Furthermore, the intensity of the laser beam is distributed radially according to a Gaussian function, which means that the total intensity of light varies with the angle of incidence. When the probe penetrates the sample, the light will no longer accumulate at the same position on the optical axis, which will cause redistribution of the axial light intensity.

The relationship between light intensity and incidence angle can be shown as

$$I(\alpha) = I_0 \xi \exp\left(-8h^2 \tan^2\alpha/d^2\right), \tag{3}$$

in which I_0 represents the total intensity of the beam, ξ is the standardized coefficient, and h and d represent the working distance and the aperture of the objective lens respectively. If the position at which α=0 is taken as the starting point, the positions of light rays of different incident angles in the sample can be expressed as

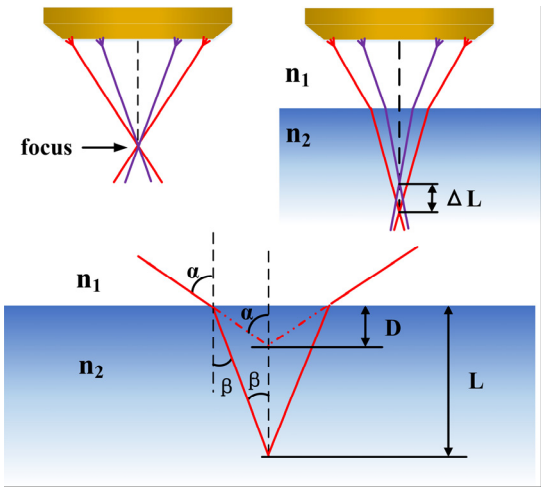

FIG. 3. Schematic diagram of ray tracing.

$$Z = D\frac{\tan\alpha}{\tan\left(\arcsin\left(n_1\sin\alpha/n_2\right)\right)} - \lim_{\alpha\to 0} D\frac{\tan\alpha}{\tan\left(\arcsin\left(n_1\sin\alpha/n_2\right)\right)} = D\frac{\tan\alpha}{\tan\left(\arcsin\left(n_1\sin\alpha/n_2\right)\right)} - D\frac{n_2}{n_1}. \quad (4)$$

The function relating light intensity and Z can be regarded as the implicit function $I_{n_2}(Z)$, and a new defocusing curve can be described as

$$T_{n_2}(Z) = I_{n_2}(Z)\otimes T(Z) = \int_{-\infty}^{\infty} I_{n_2}(Z)T(Z-\tau)\,d\tau. \quad (5)$$

After that, the extremum of this defocusing curve is obtained:

$$T_{n_2}'(Z) = I_{n_2}'(Z)\otimes T(Z) = 0. \quad (6)$$

The peak is acquired at $I_{n_2}'(Z)=0$. Combined with Eq. (4), the result for the angle corresponding to the maximum is $\alpha_{\max} = 1.302906$, and the refractive index n_2 can be accurately calculated with Eq. (2).

III. EXPERIMENT AND RESULT

In the experiment, N-BK7 glass and Silica glass with two parallel surfaces are used as samples; the scanning curve for N-BK7 glass is shown in Fig. 4. The refractive index of air is 1.0003, as calculated by the Edlen equation [29], and the reference refractive indices of the samples are derived from the interpolation formula of the ZEMAX software. The actual thickness of the sample is found by micrometer with an uncertainty of 1 μm, each sample being measured 10 times in this experiment; the average of the results is regarded as the parameter L. The parameter D is measured as the interval between the peaks of the scanning curve, each sample again being measured 10 times. After that, the refractive index can be acquired by substituting the values for D, L, and $\alpha_{\max}$ into Eq. (2). The results shown in Table 1 are in agreement with the reference values, and the difference between them is less than 0.001 in each case.

The refractive indices of multilayered media are measured in the next experiment. The conditions of an optical probe in a multilayered medium are shown in Fig. 5, where the refractive indices, inciden angle, and distance from the first surface to the focus of the incident ray for each layer are n_i, θ_i, and L_i respectively. Then, according to Snell's Law of refraction and Fig. 5, we can obtain the recursion formula

$$\begin{cases} n_i = \dfrac{n_{i-1}\sin\theta_{i-1}}{\sin\left(\arctan\left(\left(\left(L_i - \sum_{n=1}^{i-2}\Delta L_n\right)\tan\theta_{i-1}\right)\Big/\Delta L_i\right)\right)}, \\ L_i = \left(\left(L_{i-1} - \sum_{n=1}^{i-2} D_n\right)\tan\theta_{i-2}\right)\Big/\tan\theta_{i-1} - \sum_{n=1}^{i-2} D_n, \\ \theta_{i-1} = \arcsin\left(n_0\sin\theta_0/n_{i-1}\right). \end{cases} \quad (7)$$

The initial condition of the recursion formula is

$$\begin{cases} n_0 = 1.0003, \\ L_1 = \sum_{n=1}^{i} D_n, \\ \theta_0 = \alpha_{\max}. \end{cases} \quad (8)$$

in which the peak separation in the scanning curve and the physical thickness of layer i are defined as D_i and ΔL_i respectively. In this experiment, a microfluidic chip with a

TABLE 1. Refractive index measurement of N-BK7 and silica plain glass

Sample	L (mm)	D (mm)	Refractive index	
			Reference	Measurement
N-BK7 Glass1	4.992	3.2661	1.506634	1.506529
N-BK7 Glass2	4.018	2.6287	1.506634	1.506773
Silica Glass1	1.122	0.7672	1.440261	1.440409

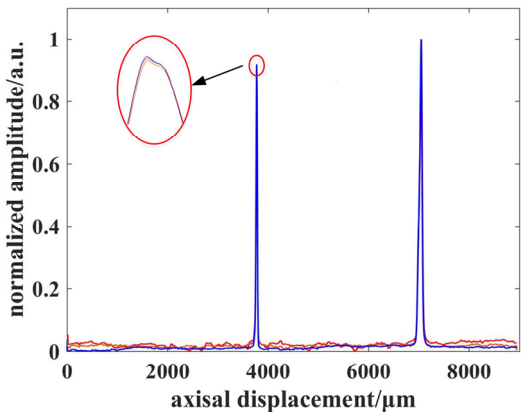

FIG. 4. Scanning curve for N-BK7 glass.

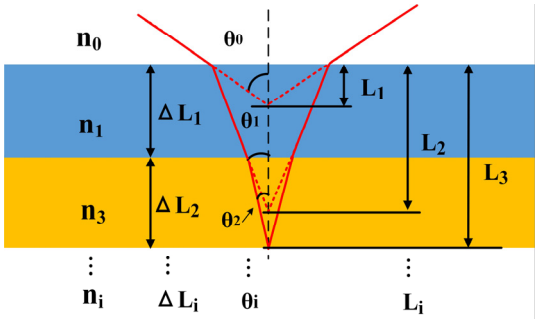

FIG. 5. Ray-tracing schematic for a multilayered medium.

4-layer structure is chosen as a sample, as shown in Fig. 6. Meanwhile, Fig. 7 displays the scanning curve along the red dotted line in Fig. 6. Then the physical thickness ΔL_i and reference refractive index of each layer are obtained from the design dimensions of the microfluidic chip, and shown in Table 2.

Finally, the refractive index of each layer can be calculated using Eqs. (7) and (8); the results are shown in Table 2. The experimental results are in agreement with the reference values given by the manufacturer. The differences between them are less than 0.005, and the stability of refractive index is better than 0.0006. The error of the refractive-index measurement is mainly caused by the imprecise physical thickness, which comes from the design dimensions. If the error in corresponding physical thickness were less than 1 μm, the corresponding uncertainty in refractive index would be less than 0.0021. Moreover, the positional-defocusing curve's peak influences the results of the experiment. The uncertainty in refractive index could be less than 0.003, if the positioning accuracy were better than 1 μm. In the experiment, the positioning accuracy of the stage is better than 1 μm, and the measurements above all indicate that the new method for refractive-index measurement of multilayered media with the laser-frequency-shifted feedback confocal microscope is effective and reliable.

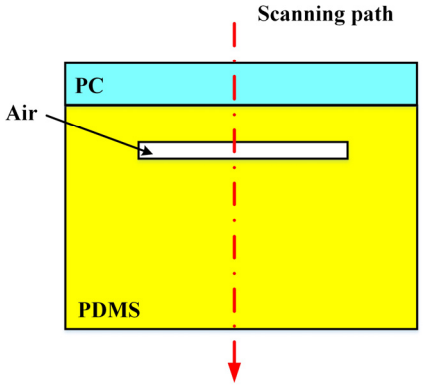

FIG. 6. Schematic of the microfluidic chip's structure.

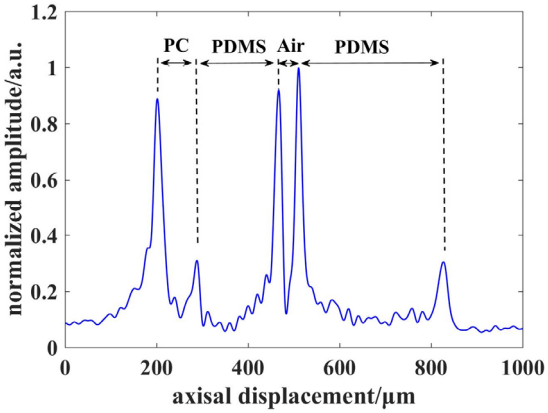

FIG. 7. Scanning curve for the microfluidic chip.

TABLE 2. Refractive-index measurements for the microfluidic chip

Layer	Physical thickness (μm)	Peak separation (μm)	Refractive index	
			Reference	Measurement
1. PC	140	86.6	1.5912	1.59328
2. PDMS	260	172.1	1.4865	1.48742
3. Air	45	44.8	1.0003	1.00454
4. PDMS	475	315.3	1.4865	1.48538

IV. CONCLUSION

In conclusion, we present a new method to measure the refractive index of single plain glass or multilayered material based on the laser frequency-shifted confocal feedback microscope. Combining the laser frequency-shift feedback technique and the confocal effect, the method can obtain high axial-positioning accuracy and sensitivity. The N-BK7 glass and Silica plain glass serve as samples, and their measured refractive indices are 1.5065 and 1.4404 respectively. According to the measured results for N-BK7 glass and Silica plain glass, the measurement uncertainty in refractive index is less than 0.001. After scanning a microfluidic chip with four layers and calculating the refractive index of each layer with a recursion formula, the feasibility of this method for multilayered materials is tested. The measured refractive indices of the PDMS layer and PC layers are 1.5932 and 1.4874 respectively, and the measurement uncertainty in refractive index is better than 0.005.

Compared to conventional methods, our system is more compact and has less difficulty in sample processing, and thus can be utilized in many settings, such as an ordinary laboratory or industry. In this work, the refractive indices of single plain glass and multilayered materials are measured at 1064 nm, which is significant for the manufacture of near-infrared optical materials. Furthermore, the presented method can be further used to measure the refractive index of a liquid, by using a microfluidic chip whose design dimensions are accurately known.

REFERENCES

1. S. Singh, "Refractive index measurement and its applications," Phys. Scr. **65**, 167-180 (2002).
2. J. W. Ye, M. Xia, and K.-C. Yang, "An improved differential algorithm for the critical-angle refractometer," Optoelectron. Lett. **15**, 108-112 (2019).
3. V. G. Plotnichenko and V. O. Sokolov, "Influence of

absorption on the refractive index determination accuracy by the minimum deviation method," Appl. Opt. **57**, 639-647 (2018).
4. G. H. Meeten, "Refractive index errors in the critical-angle and the Brewster-angle methods applied to absorbing and heterogeneous materials," Meas. Sci. Technol. **8**, 728-733 (1997).
5. C. M. Herzinger, B. Johs, W. A. McGahan, J. A. Woollam, and W. Paulson, "Ellipsometric determination of optical constants for silicon and thermally grown silicon dioxide via a multi-sample, multi-wavelength, multi-angle investigation," J. Appl. Phys. **83**, 3323-3336 (1998).
6. Y. Liang, F. Wang, X. Luo, Q. Li, T. Lin, I. T. Ferguson, Q. Yang, L. Wan, and Z. C. Feng, "Investigation of the optical properties of InSb thin films grown on GaAs by temperature-dependent spectroscopic ellipsometry," J. Appl. Spectrosc. **86**, 276-282 (2019).
7. D. Schmidt, B. Booso, T. Hofmann, E. Schubert, A. Sarangan, and M. Schubert, "Monoclinic optical constants, birefringence, and dichroism of slanted titanium nanocolumns determined by generalized ellipsometry," Appl. Phys. Lett. **94**, 011914 (2009).
8. S. Guo, G. Gustafsson, O. J. Hagel, and H. Arwin, "Determination of refractive index and thickness of thick transparent films by variable-angle spectroscopic ellipsometry: application to benzocyclobutene films," Appl. Opt. **35**, 1693-1699 (1996).
9. T. Schneider, D. Leduc, C. Lupi, J. Cardin, H. Gundel, and C. Boisrobert, "A method to retrieve optical and geometrical characteristics of three layer waveguides from *m*-lines measurements," J. Appl. Phys. **103**, 063110 (2008).
10. T. Wood, V. Brissonneau, J.-B. Brückner, G. Berginc, F. Flory, J. L. Rouzo, and L. Escoubas, "Optical measurement of exposure depth and refractive index in positive photoresists," Opt. Commun. **291**, 184-192 (2013).
11. S. Monneret, P. Huguet-Chantome, and F. Flory, "*m*-Lines technique: prism coupling measurement and discussion of accuracy for homogeneous waveguides," J. Opt. A: Pure Appl. Opt. **2**, 188-195 (2000).
12. R. Ince and E. Hüseyinoğlu, "Decoupling refractive index and geometric thickness from interferometric measurements of a quartz sample using a fourth-order polynomial," Appl. Opt. **46**, 3498-3503 (2007).
13. G. D. Gillen and S. Guha, "Use of michelson and Fabry-Perot interferometry for independent determination of the refractive index and physical thickness of wafers," Appl. Opt. **44**, 344-347 (2005).
14. S. H. Kim, S. H. Lee, J. I. Lim, and K. H. Kim, "Absolute refractive index measurement method over a broad wavelength region based on white-light interferometry," Appl. Opt. **49**, 910-914 (2010).
15. N. A. Andrushchak, O. I. Syrotynsky, I. D. Karbovnyk, Y. V. Bobitskii, A. S. Andrushchak, and A. V. Kityk, "Interferometry technique for refractive index measurements at subcentimeter wavelengths," Microw. Opt. Technol. Lett. **53**, 1193-1196 (2011).
16. H. J. Choi, H. H. Lim, H. S. Moon, T. B. Eom, J. J. Ju, and M. Cha, "Measurement of refractive index and thickness of transparent plate by dual-wavelength interference," Opt. Express **18**, 9429-9434 (2010).
17. L. Xu, S. Zhang, Y. Tan, and L. Sun, "Simultaneous measurement of refractive-index and thickness for optical materials by laser feedback interferometry," Rev. Sci. Instrum. **85**, 083111 (2014).
18. C. J. Hao, Y. Lu, M. T. Wang, B. Q. Wu, L. C. Duan, and J. Q. Yao, "Surface plasmon resonance refractive index sensor based on active photonic crystal fiber," IEEE Photonics J. **5**, 4801108 (2013).
19. L. Ji, X. Sun, G. He, Y. Liu, X. Wang, Y. Yi, and D. Zhang, "Surface plasmon resonance refractive index sensor based on ultraviolet bleached polymer waveguide," Sens. Actuator B **244**, 373-379 (2017).
20. B. Gauvreau, A. Hassani, M. F. Fehri, A. Kabashin, and M. Skorobogatiy, "Photonic bandgap fiber-based surface plasmon resonance sensors," Opt. Express **15**, 11413-11426 (2007).
21. K. Otsuka, "Effects of external perturbations on LiNdP4O12 lasers," IEEE J. Quantum. Electron. **15**, 655-663 (1979).
22. P. G. R. King and G. J. Steward, "Metrology with an optical maser," New Sci. **17**, 14 (1963).
23. S. Donati, G. Giuliani, and S. Merlo, "Laser diode feedback interferometer for measurement of displacements without ambiguity," IEEE J. Quantum. Electron. **31**, 113-119 (1995).
24. B. Ovryn and J. H. Andrews, "Phase-shifted laser feedback interferometry," Opt. Lett. **23**, 1078-1080 (1998).
25. L. Scalise, Y. Yu, G. Giuliani, G. Plantier, and T. Brosch, "Self-mixing laser diode velocimetry: application to vibration and velocity measurement," IEEE Trans. Instrum. Meas. **53**, 223-232 (2004).
26. K. Otsuka, K. Abe, J.-Y. Ko, and T.-S. Lim, "Real-time nanometer-vibration measurement with a self-mixing micro-chip solid-state laser," Opt. Lett. **27**, 1339-1341 (2002).
27. J. Li, H. Niu, and Y. X. Niu, "Laser feedback interferometry and applications: a review," Opt. Eng. **56**, 050901 (2017).
28. Y. Tan, W. Wang, C. Xu, and S. Zhang, "Laser confocal feedback tomography and nano-step height measurement," Sci. Rep. **3**, 2971 (2013).
29. K. P. Birch and M. J. Downs, "Correction to the updated Edlén equation for the refractive index of air," Metrologia **31**, 315-316 (1994).